PB83-251637

Investigation of Resonant Optoacoustic Cells

North Carolina State Univ. at Raleigh

Prepared for

Environmental Sciences Research Lab.
Researth Triangle Park, NC

Aug 83

U.S. Department of Commerce
National Technical Information Service
NTIS

TECHNICAL REPORT DATA
(Please read Instructions on the reverse before completing)

1. REPORT NO. EPA-600/3-83-070	2.
3. RECIPIENT'S ACCESSION NO. PB83 251637	
4. TITLE AND SUBTITLE AN INVESTIGATION OF RESONANT OPTOACOUSTIC CELLS	5. REPORT DATE August 1983 6. PERFORMING ORGANIZATION CODE
7. AUTHOR(S) Robert L. Plyler and Richard R. Patty	8. PERFORMING ORGANIZATION REPORT NO.
9. PERFORMING ORGANIZATION NAME AND ADDRESS Physics Dept. N. C. State Univ. Raliegh, NC 27650	10. PROGRAM ELEMENT NO. CDTA1D/01 - 0610 (FY-83) 11. CONTRACT/GRANT NO. R-805332
12. SPONSORING AGENCY NAME AND ADDRESS Environmental Sciences Research Laboratory - RTP, NC Office of Research and Development U.S. Environmental Protection Agency Research Triangle Park, N. C. 27711	13. TYPE OF REPORT AND PERIOD COVERED Interim - 1980 14. SPONSORING AGENCY CODE EPA/600/09
15. SUPPLEMENTARY NOTES	

16. ABSTRACT

A theory describing the optoacoustic signal is presented; dependence on both cell and gas parameters are given and the advantage of operating at a resonant frequency is discussed. Three elliptical cells with major axes 5.8, 12.7, and 15.2 cm (corresponding minor axes 5.5, 11.0; and 7.6 cm) were utilized as resonant optoacoustic cells. Longitudinal standing waves analagous to radial resonances for a cylindrical cell were driven by passing the beam from a CO_2 laser along one focus of the ellipse. A Knowles electret microphone (model 1754) located at the other focus of the ellipse detected the pressure variations associated with the absorption of laser radiation by the gas. Plots of optoacoustic signal vs frequency are presented for frequencies up to approximately 5500 Hz; several resonances are observed. In order to determine a minimum detectable absorption coefficient, the P(14) line of the 10.6 μm CO_2 band was used to detect absorption by dilute ethylene samples. Plots of optoacoustic signal vs concentration are presented for each cell; a minimum detectable absorption coefficient of about 3×10^{-8} cm^{-1} was obtained. Results are compared with measurements on a Helmholtz cell for which the minimum detectable absorption coefficient was about 2×10^{-7} cm^{-1}. Windowless operation was attempted, and the results indicate that further improvement is possible.

17. KEY WORDS AND DOCUMENT ANALYSIS

a. DESCRIPTORS	b. IDENTIFIERS/OPEN ENDED TERMS	c. COSATI Field/Group

18. DISTRIBUTION STATEMENT RELEASE TO PUBLIC	19. SECURITY CLASS (This Report) UNCLASSIFIED	21. NO. OF PAGES 34
	20. SECURITY CLASS (This page) UNCLASSIFIED	22. PRICE

EPA Form 2220-1 (Rev. 4-77) PREVIOUS EDITION IS OBSOLETE

PB83-251637

TYPING GUIDE SHEET
BEGIN FIRST LINE OF TEXT HERE
CENTER OF PAGE
TOP OF IMAGE AREA

EPA-600/3-83-070
August 1983

DROPPED HEAD; BEGIN SECTIONS HERE

AN INVESTIGATION OF RESONANT OPTOACOUSTIC CELLS

by

Robert R. Plyler and Richard R. Patty
Physics Department
North Carolina State University
Raleigh, N. C. 27650

R-805332-01

6-1/2"

Project Officer

William A. McClenny
Analytical Instrumentation Branch
Environmental Sciences Research Laboratory
Environmental Protection Agency
Research Triangle Park, N. C. 27711

9-1/8"

ENVIRONMENTAL SCIENCES RESEARCH LABORATORY
OFFICE OF RESEARCH AND DEVELOPMENT
U. S. ENVIRONMENTAL PROTECTION AGENCY
RESEARCH TRIANGLE PARK, NORTH CAROLINA 27711

BEGIN LAST LINE OF TEXT
BOTTOM OF IMAGE AREA; OUTSIDE DIMENSION FOR TABLES AND ILLUSTRATIONS
3/8"
PAGE NUMBER
EPA-287 (Cin.)
(4-76)

REPRODUCED BY
NATIONAL TECHNICAL
INFORMATION SERVICE
U.S. DEPARTMENT OF COMMERCE
SPRINGFIELD, VA. 22161

NOTICE

This document has been reviewed in accordance with U.S. Environmental Protection Agency policy and approved for publication. Mention of trade names or commercial products does not constitute endorsement or recommendation for use.

BEGIN FIRST LINE OF TEXT HERE
TYPING GUIDE SHEET
CENTER OF PAGE
TOP OF IMAGE AREA
DROPPED HEAD; BEGIN SECTIONS HERE

ABSTRACT

A theory describing the optoacoustic signal is presented; dependence on both cell and gas parameters are given and the advantage of operating at a resonant frequency is discussed.

Three elliptical cells with major axes 5.8, 12.7, and 15.2 cm (corresponding minor axes 5.5, 11.0, and 7.6 cm) were utilized as resonant optoacoustic cells. Longitudinal standing waves and standing waves analagous to radial resonances for a cylindrical cell were driven by passing the beam from a CO_2 laser along one focus of the ellipse. A Knowles electret microphone (model 1754) located at the other focus of the ellipse detected the pressure variations associated with the absorption of laser radiation by the gas.

Plots of optoacoustic signal vs frequency are presented for frequencies up to approximately 5500 Hz; several resonances are observed. In order to determine a minimum detectable absorption coefficient, the P(14) line of the 10.6 μm CO_2 band was used to detect absorption by dilute ethylene samples. Plots of optoacoustic signal vs concentration are presented for each cell; a minimum detectable absorption coefficient of about 3×10^{-8} cm^{-1} was obtained. Results are compared with measurements on a Helmholtz cell for which the minimum detectable absorption coefficient was about 2×10^{-7} cm^{-1}. Windowless operation was attempted, and the results indicate that further improvement is possible.

BEGIN LAST LINE OF TEXT
BOTTOM OF IMAGE AREA, OUTSIDE DIMENSION FOR TABLES AND ILLUSTRATIONS
3/8"

EPA-287 (Cin.)
(4-76)

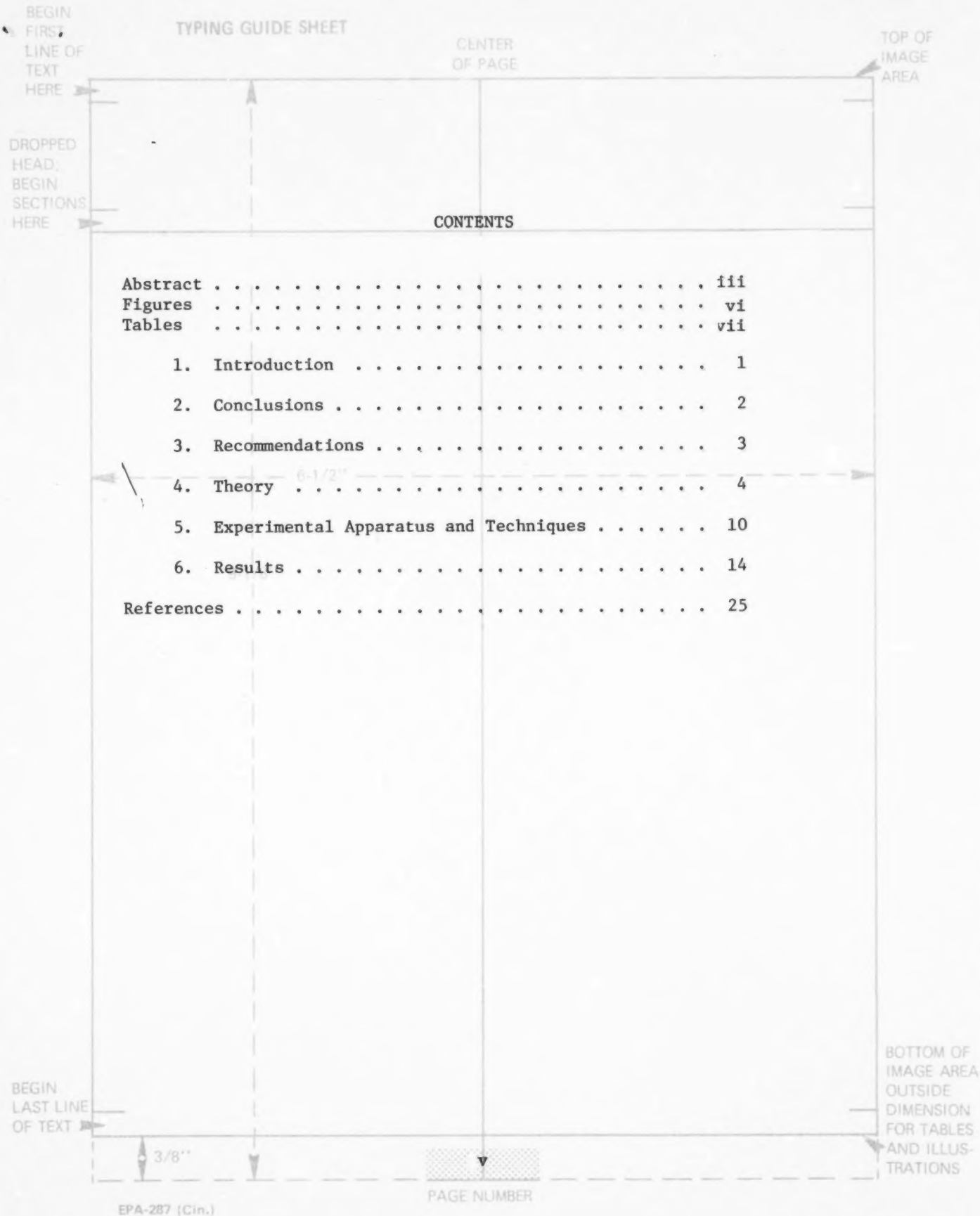

CONTENTS

Abstract iii
Figures vi
Tables vii

1. Introduction 1

2. Conclusions 2

3. Recommendations 3

4. Theory 4

5. Experimental Apparatus and Techniques 10

6. Results 14

References 25

BEGIN FIRST LINE OF TEXT HERE
TYPING GUIDE SHEET
CENTER OF PAGE
TOP OF IMAGE AREA
DROPPED HEAD; BEGIN SECTIONS HERE

FIGURES

Number		Page
1	Diagram of an elliptical cell	7
2	Diagram of a Helmholtz optoacoustic cell	8
3	Optical System	11
4	Chopper speed control circuit	12
5	Plot of signal vs frequency for elliptical cell number one using C_2H_4 in N_2	16
6	Plot of signal vs frequency for elliptical cell number one using C_2H_4 in Xe	17
7	Plot of signal vs frequency for elliptical cell number two using C_2H_4 in N_2	18
8	Plot of signal vs frequency for elliptical cell number three using C_2H_4 in N_2	19
9	Plot of signal vs concentration of C_2H_4 in N_2 using cell number three with windows	20
10	Plot of signal vs concentration of C_2H_4 in N_2 using cell number three windowless	21
11	Plot of resonant frequency vs resonator volume for the Helmholtz cell	23
12	Plot of signal vs concentration of C_2H_4 in N_2 using the Helmholtz cell	24

BEGIN LAST LINE OF TEXT
BOTTOM OF IMAGE AREA; OUTSIDE DIMENSION FOR TABLES AND ILLUSTRATIONS
3/8"

EPA-287 (Cin.)
(4-76)

BEGIN FIRST LINE OF TEXT HERE
TYPING GUIDE SHEET
CENTER OF PAGE
TOP OF IMAGE AREA
DROPPED HEAD; BEGIN SECTIONS HERE
TABLES
Number
Page
1 Solutions of Bessel's Equation . . . . . .
2 Dimensions of Various Elliptical Cells . . . . . .
3 Calculated Resonances . . . . . .
6-1/2"
9-1/8"
BEGIN LAST LINE OF TEXT
BOTTOM OF IMAGE AREA; OUTSIDE DIMENSION FOR TABLES AND ILLUSTRATIONS
3/8"
vii
PAGE NUMBER

EPA-287 (Cin.)
(4-76)

BEGIN FIRST LINE OF TEXT HERE
TYPING GUIDE SHEET
CENTER OF PAGE
TOP OF IMAGE AREA
DROPPED HEAD; BEGIN SECTIONS HERE

SECTION 1

INTRODUCTION

Over the past several years, there has been an interest in detecting very low concentrations of various pollutants. One method which holds much promise in this area involves the use of laser illuminated optoacoustic cells. These cells can be very sensitive, and extremely selective.

A major advance in optoacoustic detection occurred with the development of lasers. Previously, the only available sources of light had been thermal sources for which the output cannot exceed that of an ideal blackbody at the temperature of the source. Lasers made available very intense sources of monochromatic light which were not constrained by the limitations of thermal sources. Lasers were first used in optoacoustics by Kerr and Atwood[1] in 1968. Their experiments used both a pulsed ruby laser and a continuous operation carbon dioxide laser. Extinction coefficients as low as 1.2×10^{-7} cm^{-1} were measured.

The use of acoustically resonant chambers was reported in 1973 by Dewey, Kamm, and Hackett.[2] By utilizing standing wave amplification in the sample cell, the signal is greatly increased. The increase in signal is directly proportional to the acoustic quality or Q value of the cell and Q's of up to 1800 have been reported.[3] For simple cylindrical cells, Max and Rosengren[4] have reported a Q value of 900. The smallest extinction coefficient that has been detected is 9×10^{-9} cm^{-1} by Kritchman et. al.,[5] using a longitudinally resonant open cell. Elliptical cells could be more attractive since a lower chopping frequency can be used. [Subsequent to the completion of this work Patel and Tam published an article suggesting the use of an elliptical geometry: Appl. Phys. Lett., 36, 7 (1980)]

BEGIN LAST LINE OF TEXT
BOTTOM OF IMAGE AREA; OUTSIDE DIMENSION FOR TABLES AND ILLUSTRATIONS
3/8"

EPA-287 (Cin.)
(4-76)

BEGIN FIRST LINE OF TEXT HERE
TYPING GUIDE SHEET
CENTER OF PAGE
TOP OF IMAGE AREA
DROPPED HEAD. BEGIN SECTIONS HERE

SECTION 2

CONCLUSIONS

The results of this study show that the elliptical cell has promise as an optoacoustic detector for use in detecting low concentration pollutant gases. Using a windowless cell, it has been possible to detect slightly less than one part per billion of ethylene; this corresponds to an extinction coefficient of 2.8×10^{-8} cm^{-1}. Although this is somewhat higher than the minimum reported in the literature, improvements can be anticipated by limiting the laser noise (short term power fluctuations) and by removing the laser power meter (a source of background signal) from the chamber that encloses the elliptical cell.

Comparison of the elliptical cell with a Helmholtz resonator indicated that the elliptical cell was a factor of eight more sensitive; improvements in both cells are possible. Although some turbulence may be set up, the combination of a low flow rate and phase sensitive detection would minimize the noise associated with turbulence; thus, a system involving the flow of gas through a chamber containing a windowless cell appears feasible.

BEGIN LAST LINE OF TEXT
BOTTOM OF IMAGE AREA OUTSIDE DIMENSION FOR TABLES AND ILLUSTRATIONS
3/8"

EPA-287 (Cin.)
(4-76)

BEGIN FIRST LINE OF TEXT HERE
TYPING GUIDE SHEET
CENTER OF PAGE
TOP OF IMAGE AREA
DROPPED HEAD. BEGIN SECTIONS HERE

SECTION 3

RECOMMENDATIONS

Limited further study of resonant optoacoustic cells should be undertaken to include the following:

1. Additional measurements using resonant windowless cells which are better isolated from ambient noise and power measuring devices.

2. Measurements using resonant cells for which the laser beam enters and leaves at a pressure node.

3. Measurements using an annular resonant cell. An annular cell would support a standing wave which would be analagous to a longitudinal standing wave, but the driving radiation would be entirely located at an antinode. There is an additional advantage of low cell volume, and windowless operation is attractive.

4. Additional studies of Helmholtz cells. Various optical arrangements involving two cells could reduce window signals.

BEGIN LAST LINE OF TEXT
BOTTOM OF IMAGE AREA. OUTSIDE DIMENSION FOR TABLES AND ILLUSTRATIONS
3/8"

PAGE NUMBER
EPA-287 (Cln.)
(4-76)

BEGIN FIRST LINE OF TEXT HERE
TYPING GUIDE SHEET
CENTER OF PAGE
TOP OF IMAGE AREA
DROPPED HEAD. BEGIN SECTIONS HERE

SECTION 4

THEORY

General Theory

When a beam of radiation is incident on an absorbing gas, the molecules are excited to higher energy levels from which transitions occur to the ground state by either radiative relaxation or by other modes including collisional relaxation. If the process is dominated by collisional relaxation, the excitation energy is transferred into the translational kinetic energy of the molecules; thus an increase in pressure occurs. Periodic pressure variations occur if the incident radiation is chopped, and these variations can be detected by a sensitive microphone attached to the cell confining the gas.

The theory for the behavior of optoacoustic cells has been extensively developed by Rosengren[6,7,8,9] who derived the following expression for the pressure variation:

$$P(\omega) = \frac{Cd\bar{U}N\sigma LQ(\omega)\tau_t}{V(1 + \tau_c\tau_r^{-1})\,[1 + (\omega\tau_t)^2]^{\frac{1}{2}}\,\{1 + [\omega(\tau_c^{-1} + \tau_r^{-1})^{-1}]^2\}^{\frac{1}{2}}}$$

where C is a constant (depending on the gas), d is a constant to correct for trapezoidal chopping, $\bar{U}$ is the mean power in the cell, N is the number density of the absorbing medium, σ is the absorption cross section, L is the length of the light path through the cell, $Q(\omega)$ is the acoustic quality of the cell, τ_t is the thermal relaxation time of the cell, τ_c is the collisional relaxation time of the gas being excited, τ_r is the radiative relaxation time of the gas, V is the volume of the cell, and ω is the angular chopping frequency.

Since the thermal relaxation time for a cell, determined by the thermal diffusion to the cell wall, is typically on the order of one second at atmospheric pressure, $(\omega\tau_t)^2 >> 1$ for all frequencies greater than approximately twenty Hertz; thus, $[1 + (\omega\tau_t)^2]^{\frac{1}{2}} \simeq \omega\tau_t$. It should be noted that at lowered pressures, the diffusion time decreases; therefore, the thermal relaxation time can decrease significantly.

Although it is not always true, the radiative relaxation time is usually much greater than the collisional relaxation time. If $\tau_c\tau_r << 1$, then $(\tau_c^{-1} + \tau_r^{-1})^{-1} \simeq \tau_c$. Also, the collisional relaxation time for most gases at atmospheric pressure is on the order of 10^{-6} seconds, thus, for frequencies below approximately five kiloHertz, $(\omega\tau_c)^2 << 1$. By making the

BEGIN LAST LINE OF TEXT
BOTTOM OF IMAGE AREA OUTSIDE DIMENSION FOR TABLES AND ILLUSTRATIONS
3/8"

EPA-287 (Cin.)
(4-76)

BEGIN FIRST LINE OF TEXT HERE
TYPING GUIDE SHEET
CENTER OF PAGE
TOP OF IMAGE AREA
DROPPED HEAD; BEGIN SECTIONS HERE

above approximations in equation (1), the optoacoustic signal for most gases, for a range of from twenty Hertz to five kiloHertz, can be expressed as:

$$P(\omega) = \frac{C\bar{d}UN\sigma LQ(\omega)}{V\omega} \qquad (2)$$

As can be seen from this equation, the signal should be directly proportional to the density of the absorber, the absorption coefficient, the power in the beam, the length of the path over which the light travels, and the acoustic quality. All these factors affect the signal linearly, as should be expected. The signal is also inversely proportional to cell volume and chopping frequency. The inverse dependence on frequency is easily visualized since the temperature rise should be directly proportional to the time that the gas is exposed to the beam. Also, the inverse dependence on volume is expected because a larger volume would require a larger amount of radiation to be absorbed to generate equivalent temperature rises.

The source of illumination usually used in optoacoustic experiments is a laser. Lasers, not being limited to emitting only as a blackbody, offer large amounts of power over a very narrow bandwidth. The fact that lasers generally offer only a discrete band of wavelengths would be a disadvantage in conventional spectroscopy, but emission at discrete wavelengths is an advantage in optoacoustic spectroscopy if by chance, particular laser wavelenghts correspond to absorption peaks in the sample spectrum; in this case, very strong and consistently reproducible absorption coefficients are observed.

One problem with optoacoustic cells does arise due to a signal arising at the interface between the window of the cell and the interior of the cell. This signal results from the heating of the window and the subsequent diffusion of this heat to the interior of the cell, where the pressure increase is detected by the microphone. By placing the cell in a large container (for acoustical isolation) and operating the cell without a window, it is possible to avoid a window signal in a manner first used by Bruce et. al.[10]

Resonant Cells

As can be seen in equation (2), the magnitude of the optoacoustic signal has an inverse frequency dependence. As both room noise and electronic noise are generally decreasing functions of frequency, the signal to noise ratio and, hence, minimum detectability may improve when chopping at the higher frequencies necessary for resonant operation. By chopping at these higher frequencies, it becomes possible to use standing wave amplification to increase the signal, similar to the manner in which the sound in an organ pipe is intensified.

There are several other advantages to using resonant cells other than amplification. Because of the larger volume to surface ratio, effects from absorption of species of interest on the cell walls can be reduced. Also, resonant cells can be operated without windows in a manner similar to that suggested by Bruce. However, windowless operation is accompanied by a reduction in Q and, thus, by a reduced optoacoustic signal. Also, an increase in the signal to noise is possible because the window signal is not

BEGIN LAST LINE OF TEXT
BOTTOM OF IMAGE AREA; OUTSIDE DIMENSION FOR TABLES AND ILLUSTRATIONS
3/8"

EPA-287 (Cln.)
(4-76)

BEGIN FIRST LINE OF TEXT HERE
TYPING GUIDE SHEET
CENTER OF PAGE
TOP OF IMAGE AREA
DROPPED HEAD; BEGIN SECTIONS HERE
6-1/2"
9-1/8"

present.

Elliptical Cells

The elliptical cell (Figure 1) is arranged so that the cell is illuminated at one focus. In a manner similar to that observed by Goldan and Goto[11] for a cylindrical cell, this cell will experience resonances when

$$f = v_s[(\alpha_{m,n}/2M)^2 + (p/2L)^2]^{\frac{1}{2}} \quad (3)$$

where $\alpha_{m,n}$ is the solution to Bessel's equation, m is the elliptical mode number, n is the azimuthal mode number, p is the longitudinal mode number, M is the length of the major axis of the cell, L is the length of the cell, and v_s is the velocity of sound. As the elliptical cell should not experience azimuthal modes, n will always be zero. Values for $\alpha_{m,n}$ are given in Table 1.

Table 1. Solutions of Bessel's Equation

m	$\alpha_{m,0}$
0	0
1	1.2197
2	2.2331
3	3.2383
4	4.2411

An advantage of the elliptical cell over the cylindrical cell is seen in equations (2) and (3). The optoacoustic signal is inversely proportional to the chopping frequency and the resonant frequencies for the elliptical cells are lower than those for the cylindrical cell of comparable dimensions. For a given frequency the signal for an elliptical cell will be more than four times that of the cylindrical cell due to the differences in cell volume; the frequency is inversely proportional to the diameter of a cylinder and to twice the major axis of an ellipse.

Helmholtz Cells

The Helmholtz cell is a simple nonresonant cell with a Helmholtz resonator attached to a side of the cell (Figure 2). In examining the properties of the Helmholtz cell, a method may be used similar to that given by Rayleigh[12] where the cell is considered to consist of two separate volumes connected by a tube. The kinetic energy of the gas traveling in the tube is given by:

$$T = 1/2(\rho\dot{X}^2/C) \quad (4)$$

where ρ is the density of the gas, X is the product of the cross sectional

BEGIN LAST LINE OF TEXT
BOTTOM OF IMAGE AREA; OUTSIDE DIMENSION FOR TABLES AND ILLUSTRATIONS
3/8"

EPA-287 (Cin.)
(4-76)

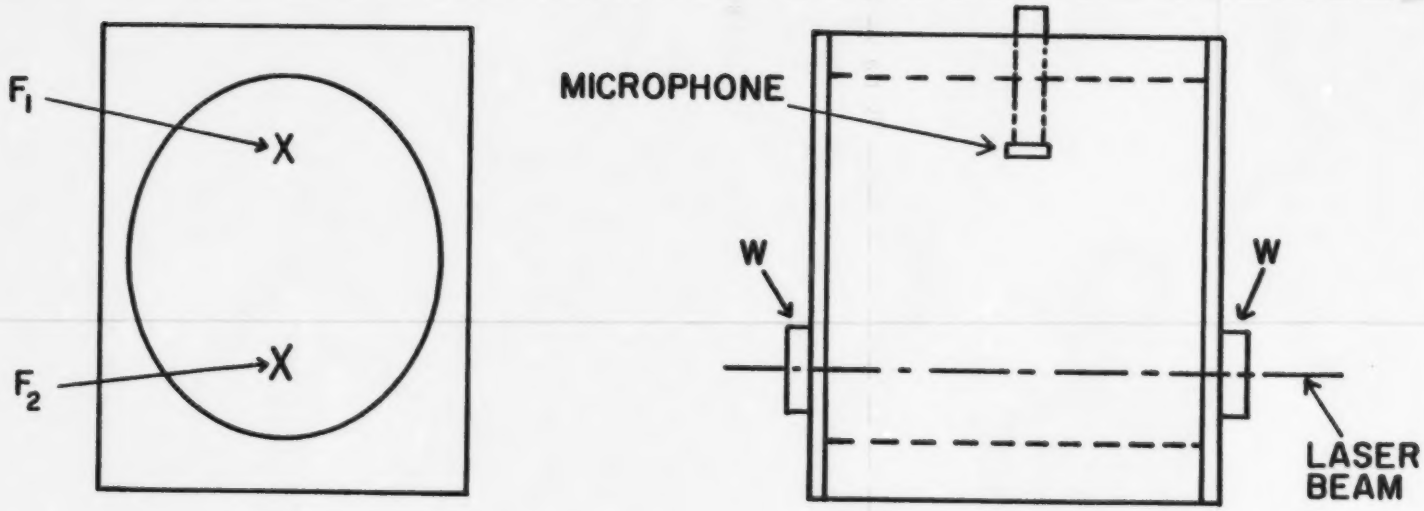

Figure 1. Diagram of an elliptical cell.

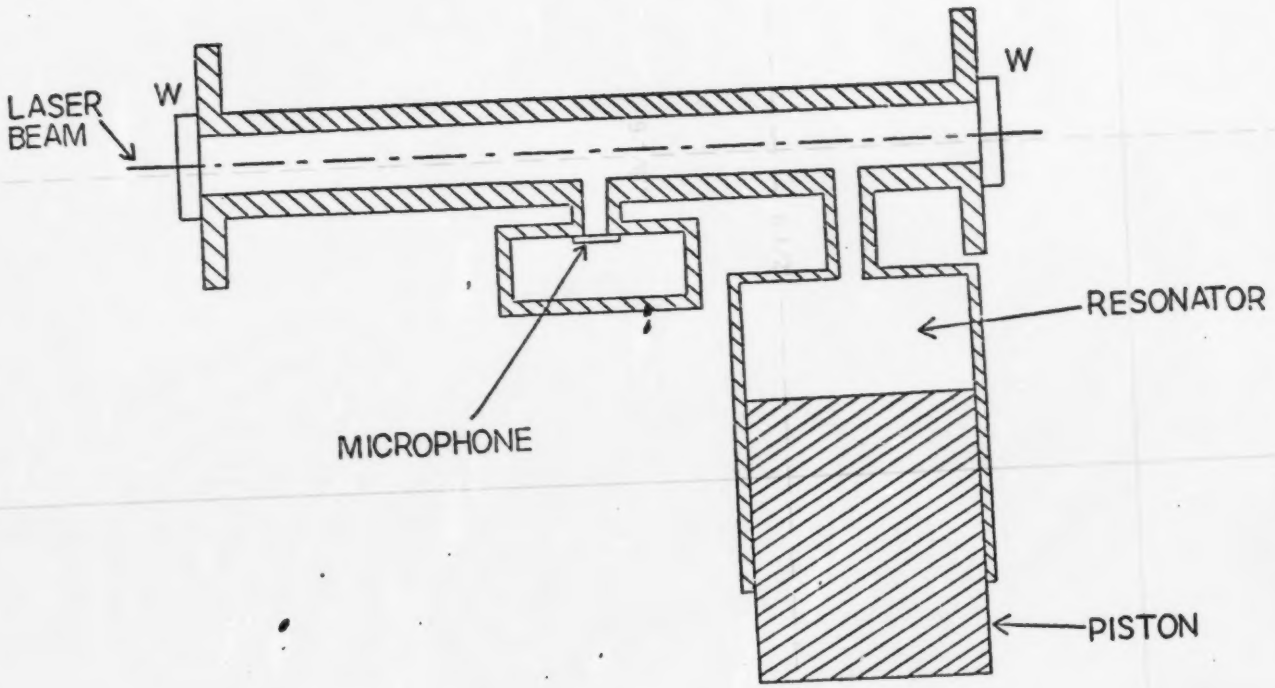

Figure 2. Diagram of a Helmholtz optoacoustic cell.

area of the connecting tube and the displacement from equilibrium, and C is the conductance of the tube. The potential energy is the sum of the potentials in both chambers:

$$\Phi = 1/2\ \rho v_s^2 X^2 (1/V_1 + 1/V_2) \tag{5}$$

where v_s is the speed of sound. The Lagrangian for this system is given by

$$L = 1/2\ \rho[\dot{X}^2/C - X^2 v_s^2 (V_1 + V_2)/V_1 V_2], \tag{6}$$

and the resulting equation of motion is

$$\ddot{X}/C + v_s^2 X(V_1 + V_2)/V_1 V_2 = 0 \tag{7}$$

Assuming X in the form $Ae^{i\omega t}$ and solving for the resonant frequency ω, we obtain

$$\omega = v_s \sqrt{C}\ [(V_1 + V_2)/V_1 V_2]^{1/2}\ . \tag{8}$$

The conductance in the tube is extremely difficult to obtain exactly. However, according to Rayleigh,[12] it can be approximated by

$$C = \pi R^2/(L + 1.7R) \tag{9}$$

where R is the radius of the tube and L is the length. For this value of conductance, the resonant frequency can be expressed as:

$$f = v_s/2\pi\ [\pi R^2 (V_1 + V_2)/V_1 V_2 (L + 1.7R)]^{1/2}\ . \tag{10}$$

BEGIN FIRST LINE OF TEXT HERE
TYPING GUIDE SHEET
CENTER OF PAGE
TOP OF IMAGE AREA
DROPPED HEAD; BEGIN SECTIONS HERE

SECTION 5

EXPERIMENTAL APPARATUS AND TECHNIQUES

The apparatus used in evaluating the various cells is shown in Figure 3. The CO_2 laser is a three meter continuous flow system which uses NaCl windows mounted at Brewster's angle. The lasing cavity is formed with a gold surfaced mirror of 10 m radius of curvature located at M_1 and a diffraction grating blazed at 10.6 μm located at M_2. By rotating the grating, approximately 80 different laser wavelengths in the 9.6 μm and the 10.6 μm bands can be selected. The radiation is taken from the laser at the zeroth order of the diffraction grating and, via flat mirror M_3, passed through a PAR model 192 light chopper. From the chopper, the radiation passes through a cell of interest to a Scientech model 36-0001 power meter where the power is monitored. A typical power entering the cell was 0.25 watt.

The optoacoustic signal in the cell is detected by a small electret microphone (in both the elliptical cells and the Helmholtz cell the microphone was a Knowles model 1754). The signal from the microphone is sent to a PAR model 128A lock-in amplifier, along with a reference signal from the chopper. The output from the lock-in amplifier is recorded on a Honeywell Electronik 19 strip chart recorder.

For some experiments, the speed control of the chopper was inadequate for a study of the extremely narrow resonances. So that the chopping frequency could be more closely controlled, a fine control for the chopper was constructed (Figure 4). With this control, it was possible to control the chopper to within approximately 0.1 Hertz. An integrated circuit oscillator, 555 (Fairchild), is made to oscillate at the approximate frequency by using various values of R_1, R_2 and C, and the frequency is fine tuned with the potentiometer P. The phase difference between the oscillator and the reference signal is measured with an exclusive OR gate in the 4046 (Fairchild) integrated circuit. This difference signal is low pass filtered; then the magnitude of this signal is lowered by the 10^6 ohm resister and applied to the external speed control of the chopper.

The P(14) laser line of the 10.6 μm band was used in evaluating these cells since ethylene has a strong absorption at this wavelength and the absorption coefficient of ethylene for this line is known to be 29.10 atm^{-1} cm^{-1} as determined by Patty et. al.(13)

Samples were prepared in two ways. For fairly large concentrations (greater than about 1ppm) known quantities of pure ethylene were injected into a mixing bag along with appropriate amounts of nitrogen or Xenon to a

BEGIN LAST LINE OF TEXT HERE
BOTTOM OF IMAGE AREA OUTSIDE DIMENSION FOR TABLES AND ILLUSTRATIONS
3/8"

PAGE NUMBER
EPA-287 (Cln.) (4-76)

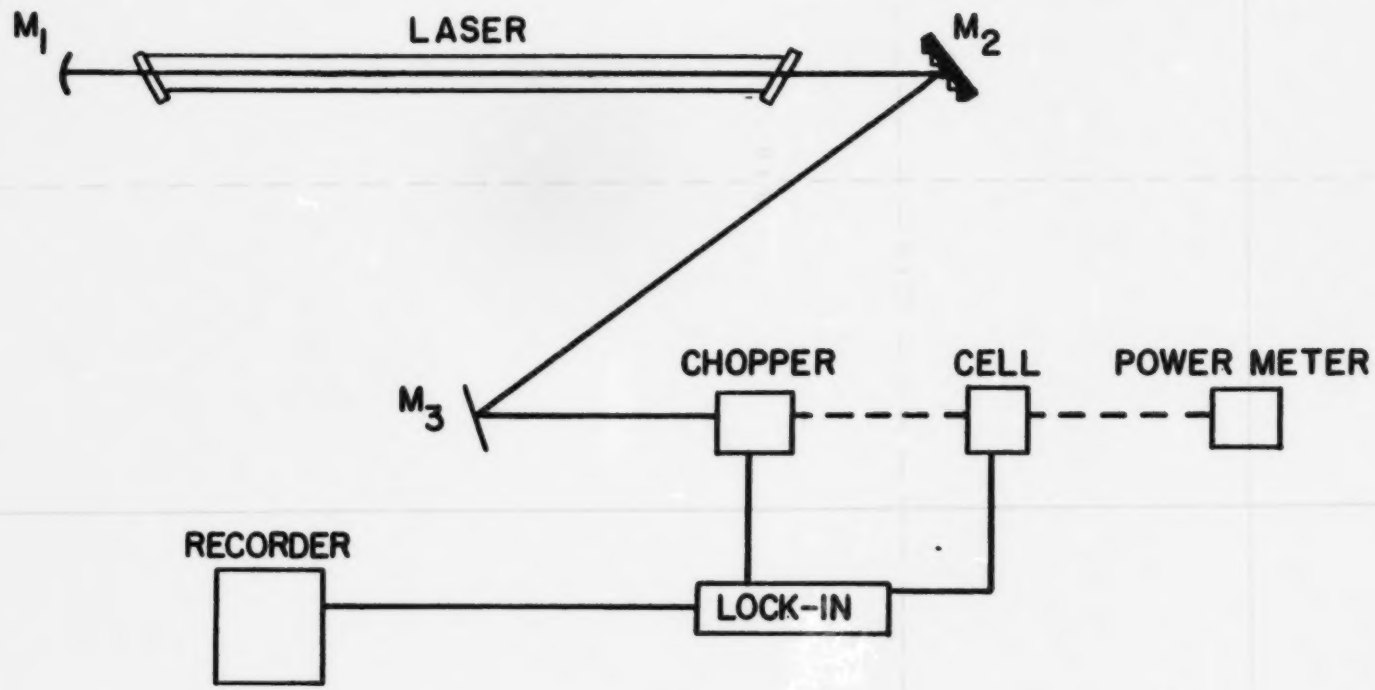

Figure 3. Optical System

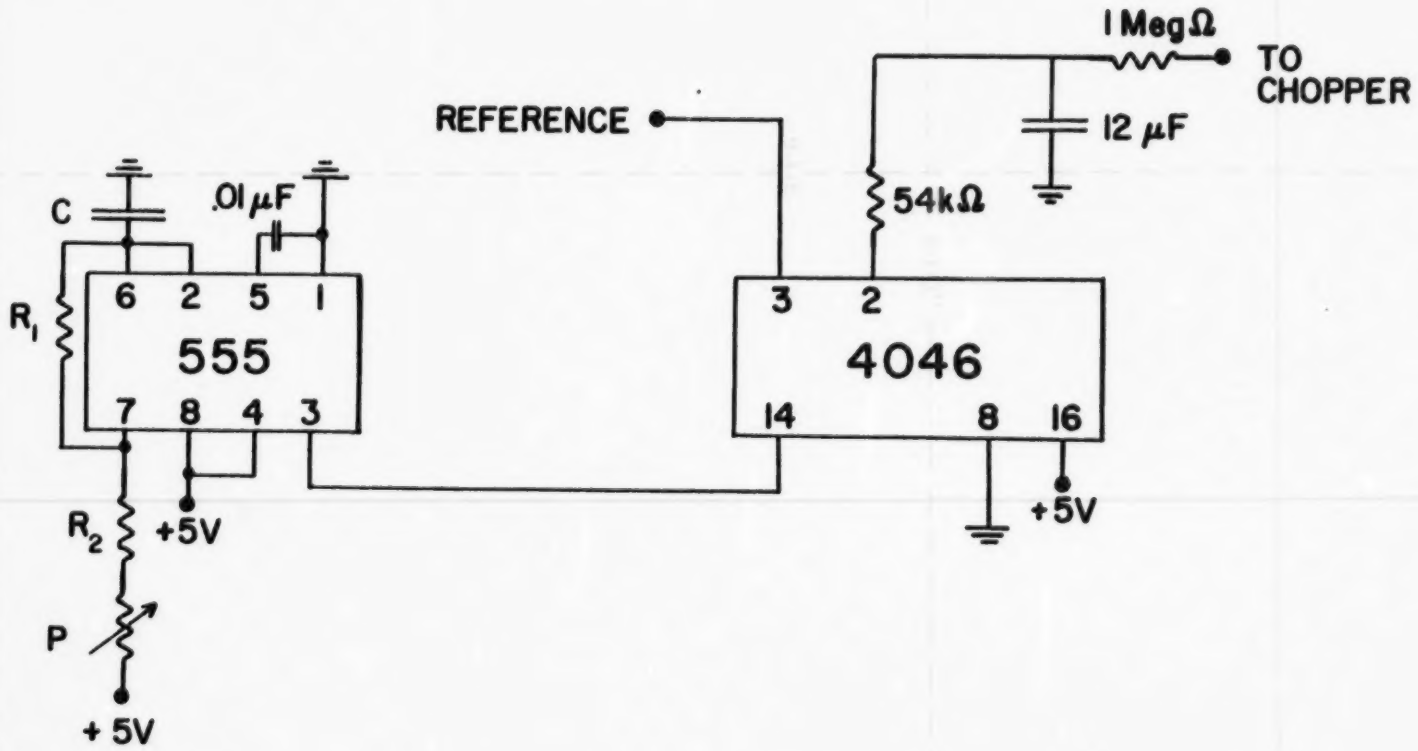

Figure 4. Chopper speed control circuit.

total pressure of 1 atm. For smaller concentrations a two stage process was employed. By first preparing a sample as above, known quantities from this bag were injected into a mixing bag, and the sample was further diluted with nitrogen or Xenon. In this manner, fairly consistent lower concentrations could be obtained. Concentrations were accurate to about ten percent; dilutions of a given concentration were more accurately determined. The purpose of using Xenon in this cell is to lower the resonant frequencies; the speed of sound in Xenon is approximately one-half that in nitrogen.

In order to evaluate the windowless elliptical cell, it was placed in a 20 liter aluminum box which was lined with foam. Radiation entered the box through a NaCl window, passed through the windowless cell and was monitored by a power meter located in the box behind the cell. When the cell was operated outside the box, NaCl windows were attached directly to the cell.

BEGIN FIRST LINE OF TEXT HERE
TYPING GUIDE SHEET
CENTER OF PAGE
TOP OF IMAGE AREA
DROPPED HEAD; BEGIN SECTIONS HERE

SECTION 6

RESULTS

Three elliptical cells were evaluated; their dimensions are listed in Table 2. The calculated resonant frequencies for single mode oscillations are listed in Table 3, and for cell number one the frequencies are also listed with Xenon being the diluting gas. All cells were aluminum.

Table 2. Dimensions of Various Elliptical Cells

Cell	Major Axis (cm)	Minor Axis (cm)	Length (cm)
1	5.8	5.5	8.9
2	12.7	11.0	15.2
3	15.2	7.6	15.2

Table 3. Calculated Resonances

Mode	Cell 1		Cell 2	Cell 3
m,p	N_2	Xe		
0,1	1932	966	1132	1132
0,2	3864	1932	2264	2264
0,3	5796	2989	3396	3396
0,4	7728	3864	4528	4528
0,5	9660	4830	5660	5660
0,6	11592	5796	6792	6792
1,0	3617	1808	1652	1380
2,0	6622	3311	3024	2527
3,0	9604	4802	4386	3665
4,0	12577	6289	5743	4800

BEGIN LAST LINE OF TEXT
BOTTOM OF IMAGE AREA; OUTSIDE DIMENSION FOR TABLES AND ILLUSTRATIONS
3/8"

EPA-287 (Cin.)
(4-76)

BEGIN FIRST LINE OF TEXT HERE
TYPING GUIDE SHEET
CENTER OF PAGE
TOP OF IMAGE AREA
DROPPED HEAD; BEGIN SECTIONS HERE

Figure 5 shows the frequency response for cell 1 with a sample of 706 ppm ethylene in nitrogen. As can be seen, the signal at the first elliptical resonance is not as large as the low frequency signal and there is not good agreement with the calculated frequency; the acoustic quality, determined by dividing the resonant frequency by the width at half maximum, is about 30. The microphone was located near the end wall for cell 1.

Figure 6 shows the frequency response of this same cell when the absorber is ethylene in Xenon. The resonant frequencies are seen to be lowered by approximately the correct amount. Because of the tendency of the Xenon atoms to diffuse through the cell joints, the frequenices of the resonances shifted slightly with time. The microphone was located closer to the wall, and the magnitude of the first longitudinal mode is seen to be larger than that of the first elliptical mode, the microphone being closer to an antinode of this resonance. The most prominent resonance appears to be the sixth longitudinal mode, having a Q of about 100. A few resonances are observed that are unexplained; possibly, they arise from mixed mode oscillations.

Figure 7 shows the frequency response for cell 2. The microphone in both this cell and cell 3 are located midway between the end walls of the cell, at a node of the first longitudinal resonance; thus, these resonances should not be observed. The first elliptical resonance is seen to be much stronger than in the smaller cell and exhibited a resonant Q of about 180. Again, there are several unexplained resonances, the most obvious being the two pairs of doublets.

The frequency response for cell 3 is shown in Figure 8. This cell exhibited the greatest normalized signal, having a Q at the first elliptical resonance of about 240. Only one unexplained resonance was observed. This cell was chosen for determining the minimum detectable concentration because of its high normalized signal.

Figure 9 shows the signal vs concentration measurements made with this cell for the lowest resonant frequency. All signals have been normalized to a power of 0.24 watts. A small airborne signal emanating from the chopper was detected by the microphone in the cell. Because this chopper signal was very stable, it did not interfere significantly with the optoacoustic signal, and its value was subtracted from all data points. After subtracting the chopper signal, a background signal, believed to originate at the cell's windows, was found. From extending the linear function of the higher concentrations (the lower trace), this signal was found to correspond to a level of about 35 parts per billion. By adding this constant signal to the lower trace, the experimentally observed upper trace is obtained. This background signal, along with noise from the laser tends to limit detectable concentrations to approximately one part per billion.

Figure 10 shows the signal vs concentration measurements made using this same cell without windows. Although the signal level was reduced to about one-third of the previous level, the background signal was reduced by a greater amount, corresponding to a concentration of about 30 parts per

BEGIN LAST LINE OF TEXT
BOTTOM OF IMAGE AREA; OUTSIDE DIMENSION FOR TABLES AND ILLUSTRATIONS
3/8"

EPA-287 (Cin.)
(4-76)

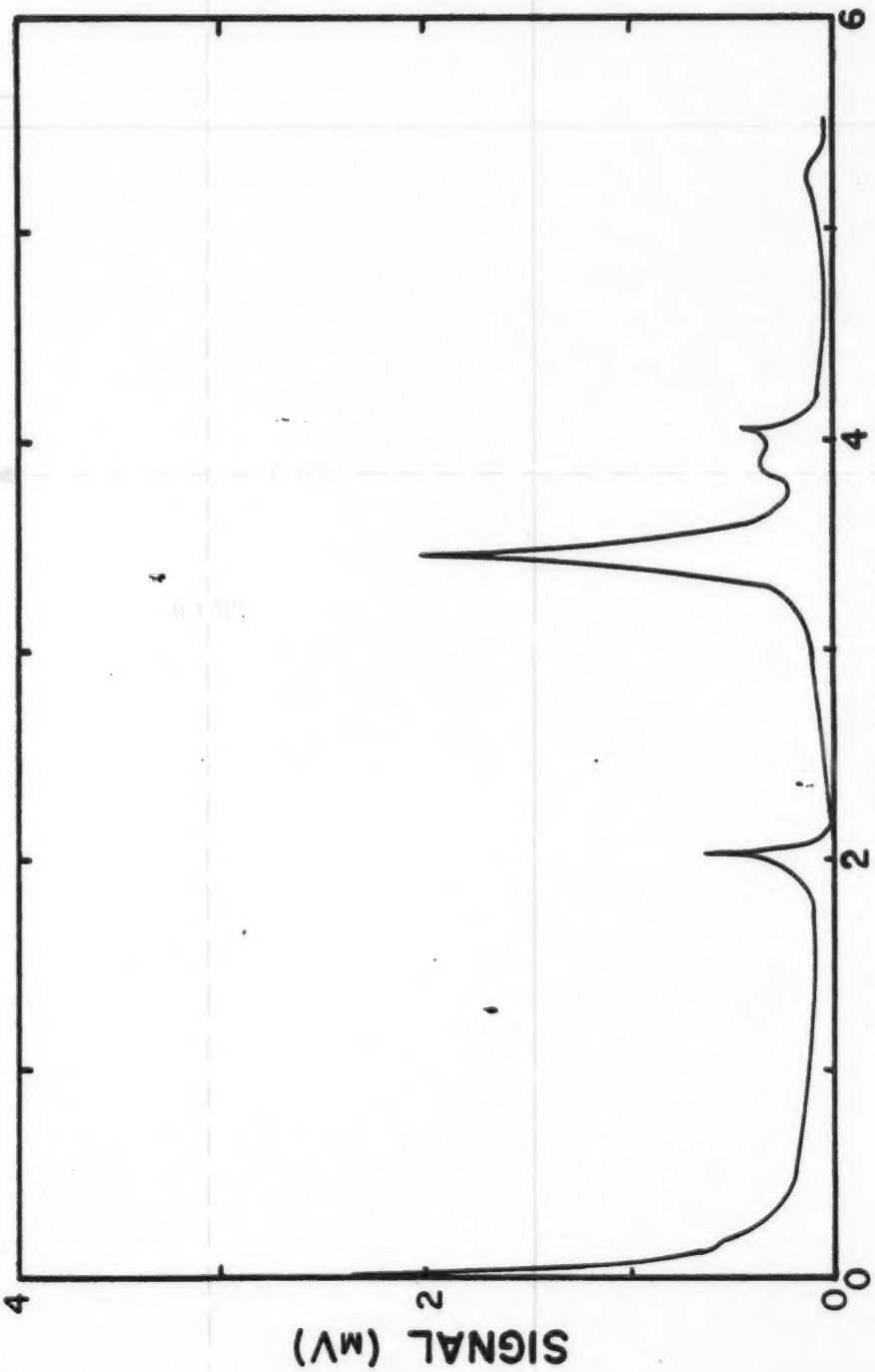

Figure 5. Plot of signal vs frequency for elliptical cell number one using C_2H_4 in N_2.

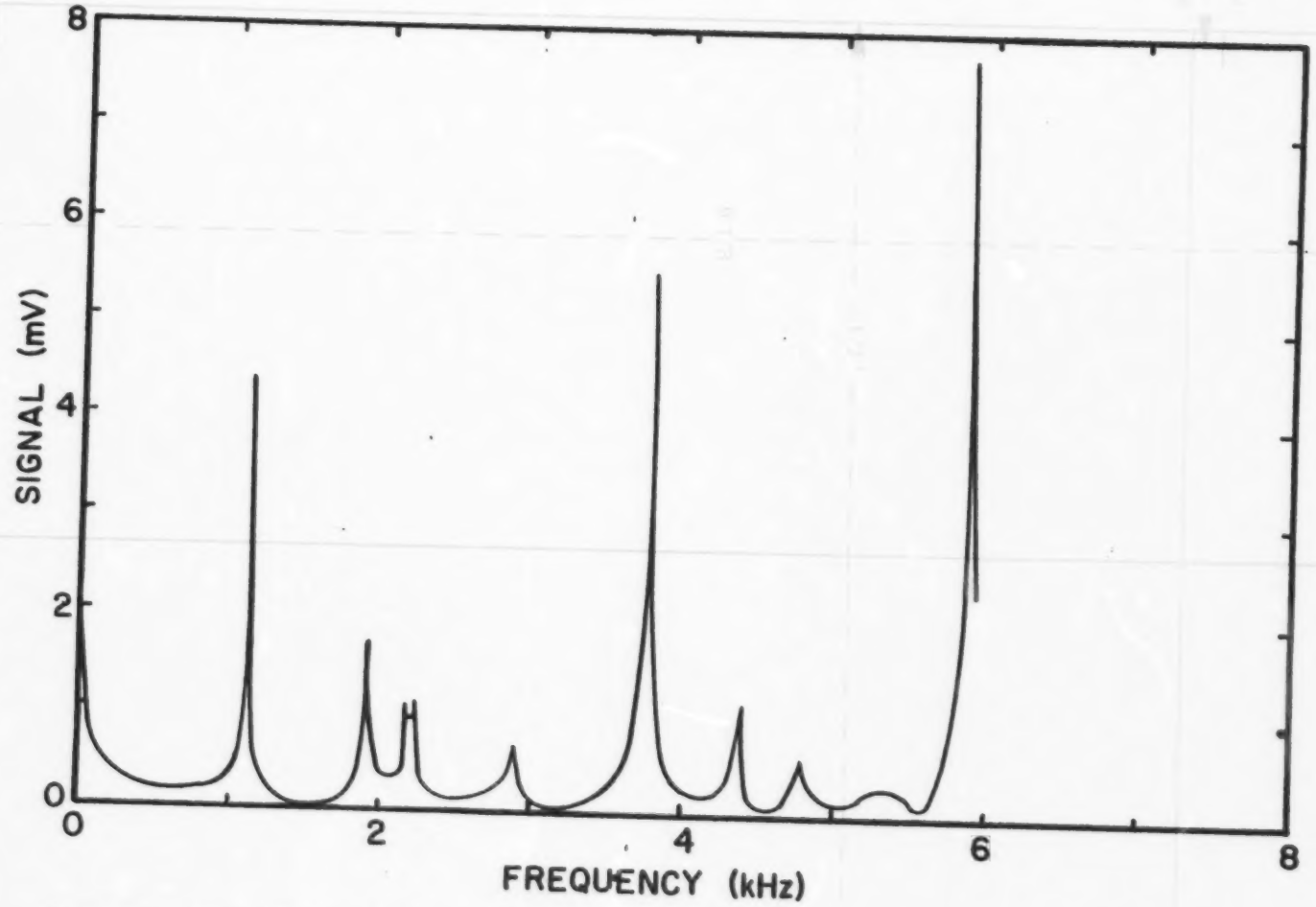

Figure 6. Plot of signal vs frequency for elliptical cell number one using C_2H_4 in Xe.

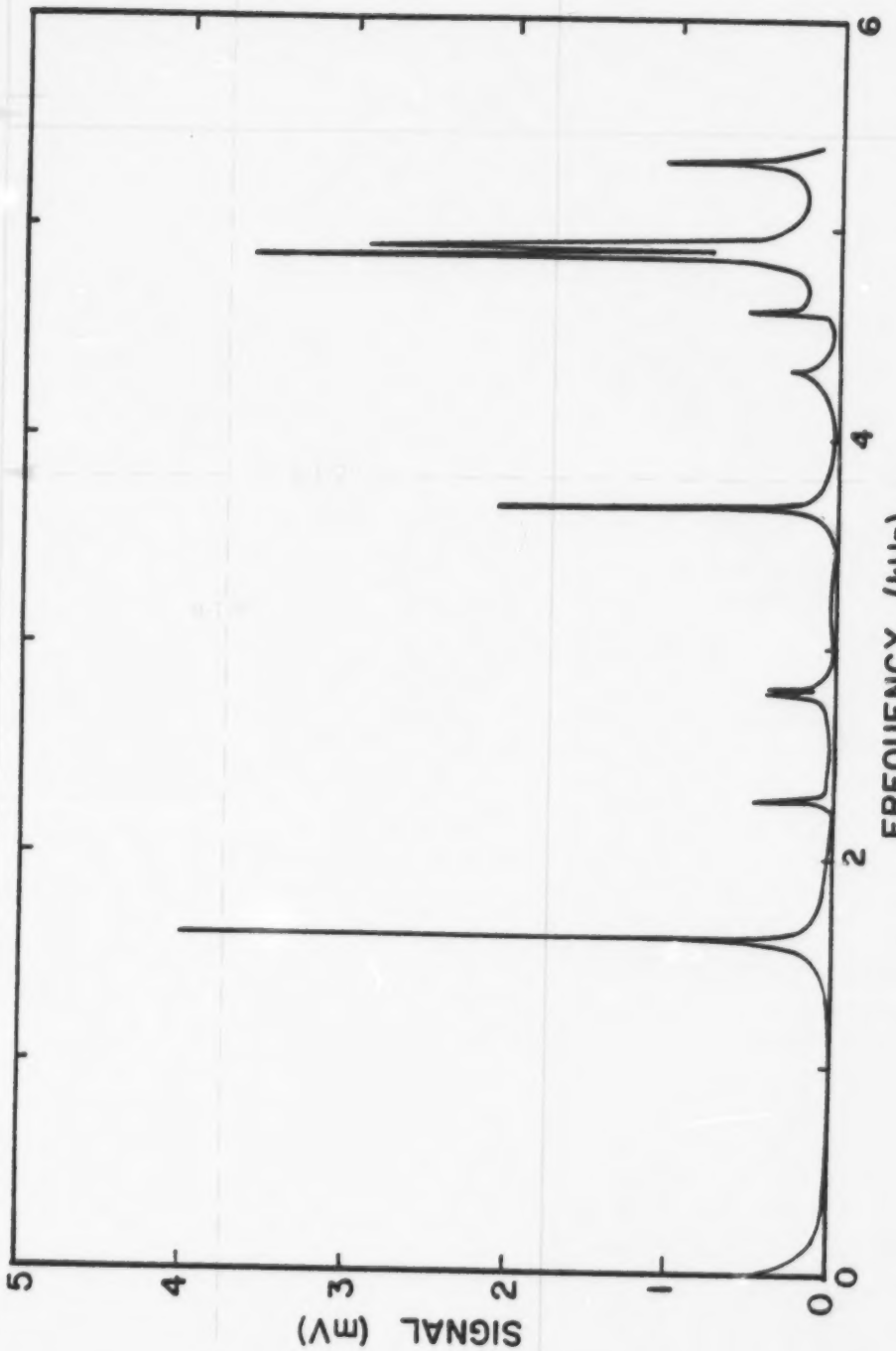

Figure 7. Plot of signal vs frequency for elliptical cell number two using C_2H_4 in N_2.

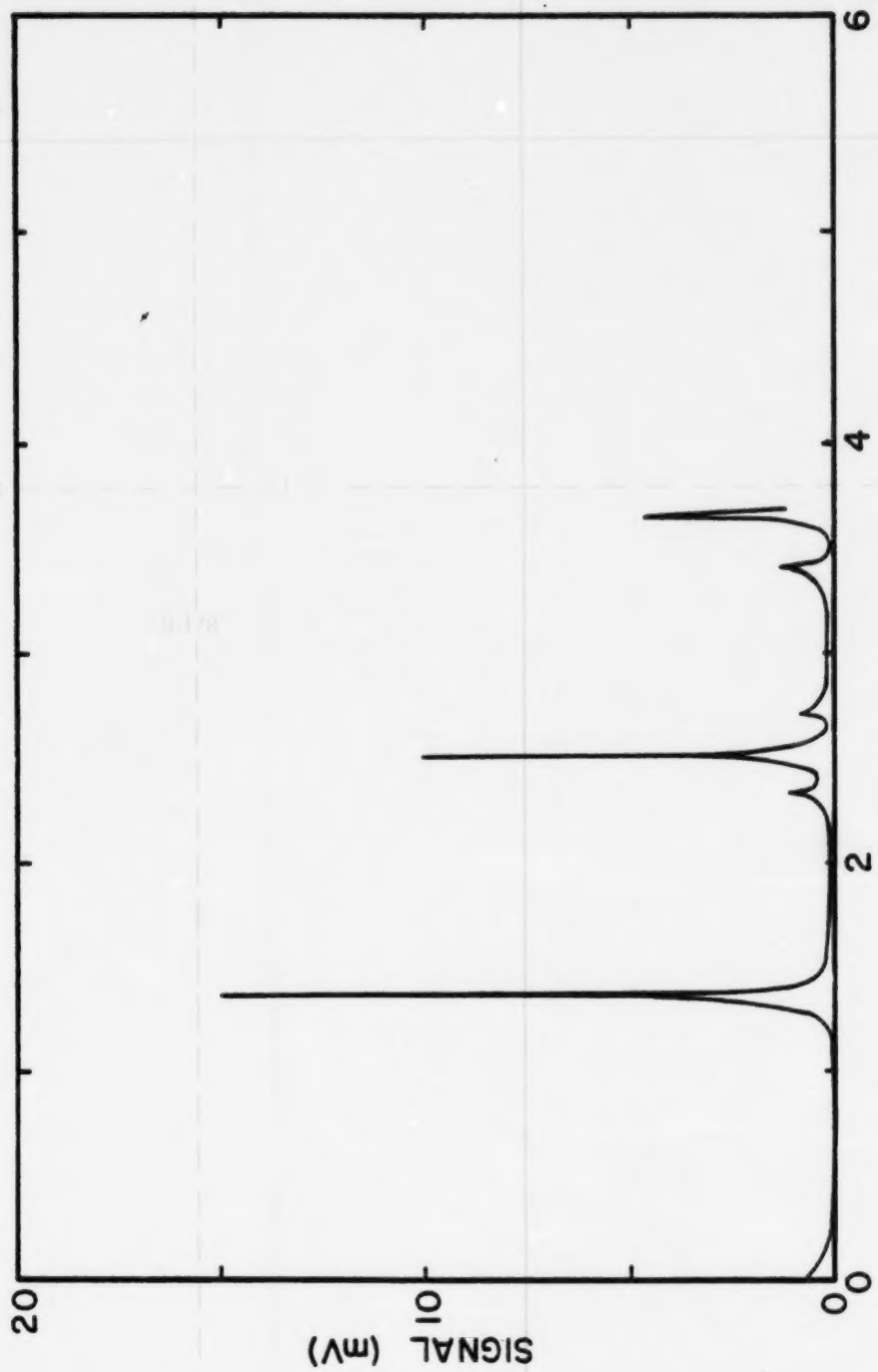

Figure 8. Plot of signal vs frequency for elliptical cell number three using C_2H_4 in N_2.

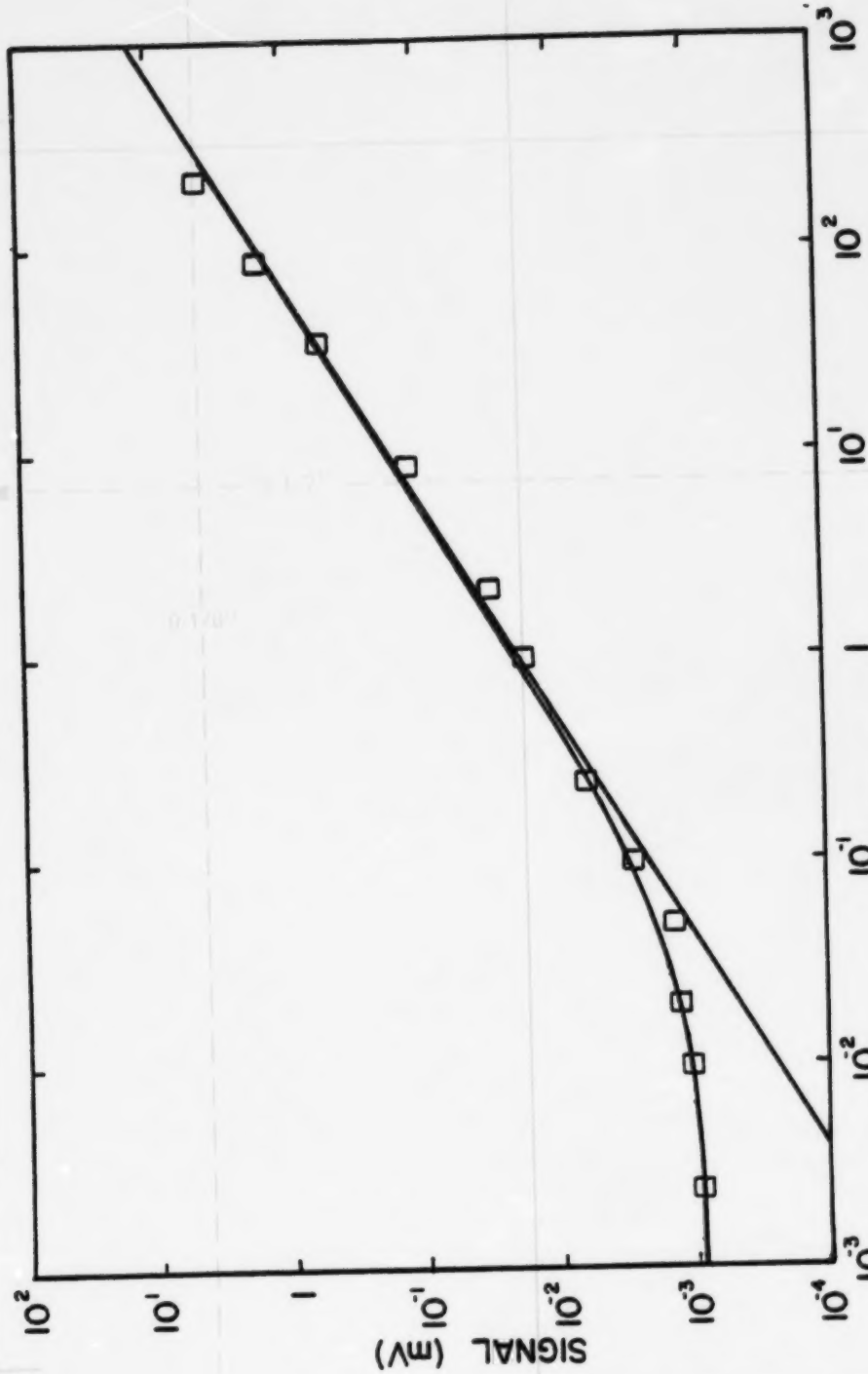

Figure 9. Plot of signal vs concentration of C_2H_4 in N_2 using cell number three with windows.

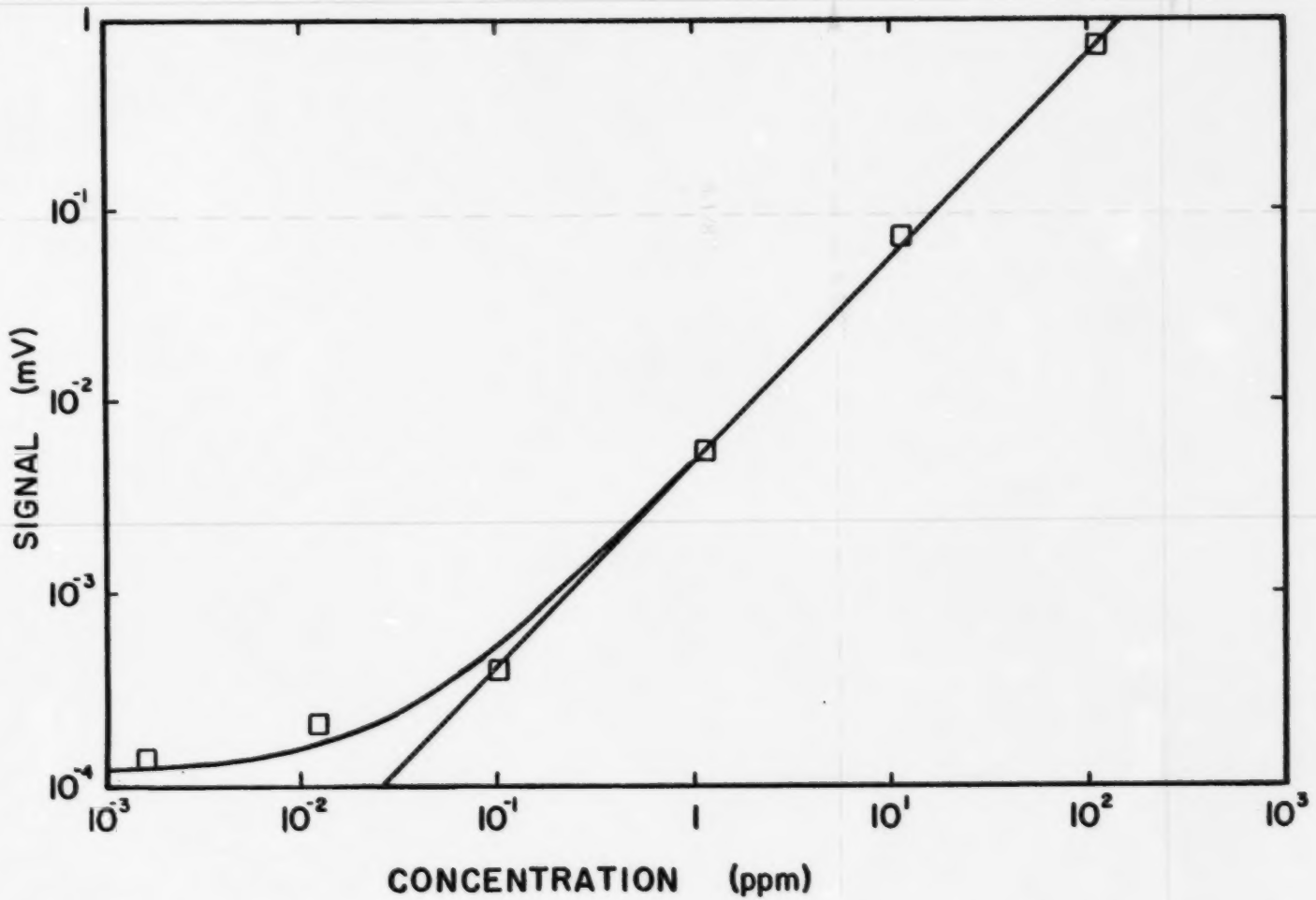

Figure 10. Plot of signal <u>vs</u> concentration of C_2H_4 in N_2 using cell number three windowless.

BEGIN FIRST LINE OF TEXT HERE
TYPING GUIDE SHEET
CENTER OF PAGE
TOP OF IMAGE AREA
DROPPED HEAD; BEGIN SECTIONS HERE

billion. This residual signal is believed to originate at the power meter located in the box. Because of the acoustic isolation provided by the box, the acoustic noise from the chopper was reduced significantly, almost becoming negligible. This method proved slightly more sensitive than the previous method, with the minimum detectable concentration being slightly under the part per billion range.

The Helmholtz cell had a main body volume of 12.31 cm^3 and the volume of the resonator could be varied, by means of a movable piston, from zero to 114 cm^3. These two cavities are connected through a tube 0.244 cm in diameter and 3.59 cm long. The acoustic quality of this cavity was measured to be about 10 for all resonator volumes greater than about 50 cm^3.

A plot of the resonant frequency vs resonator volume is shown in Figure 11. Equation (10) gives a resonant frequency at the largest volume of 355 Hertz, which is larger than the observed resonance of 305 Hertz by about 15%. Using a single measured resonant frequency to determine the conductance given by Equation (9), one obtains the solid curve for the plot of resonant frequency vs resonator volume shown in Figure 11. As can be seen, it follows the experimental data quite well.

Figure 12 shows a plot of the signal vs concentration for the Helmholtz cell at 114 cm^3. Great care was taken to assure that the radiation did not come in contact with the walls of the cell. However, a very large background signal, originating either at the windows or from light scattered from the windows onto the walls, was observed. This background signal corresponded to a concentration of 270 parts per billion and limited the minimum detectable concentration to approximately 8 parts per billion.

Although the background signals were dominant for very low concentrations, flushing the cells with N_2 and noting the change in signal allowed the determination of the minimum detectable levels given above.

BEGIN LAST LINE OF TEXT
BOTTOM OF IMAGE AREA; OUTSIDE DIMENSION FOR TABLES AND ILLUSTRATIONS
3/8"

EPA-287 (Cin.)
(4-76)

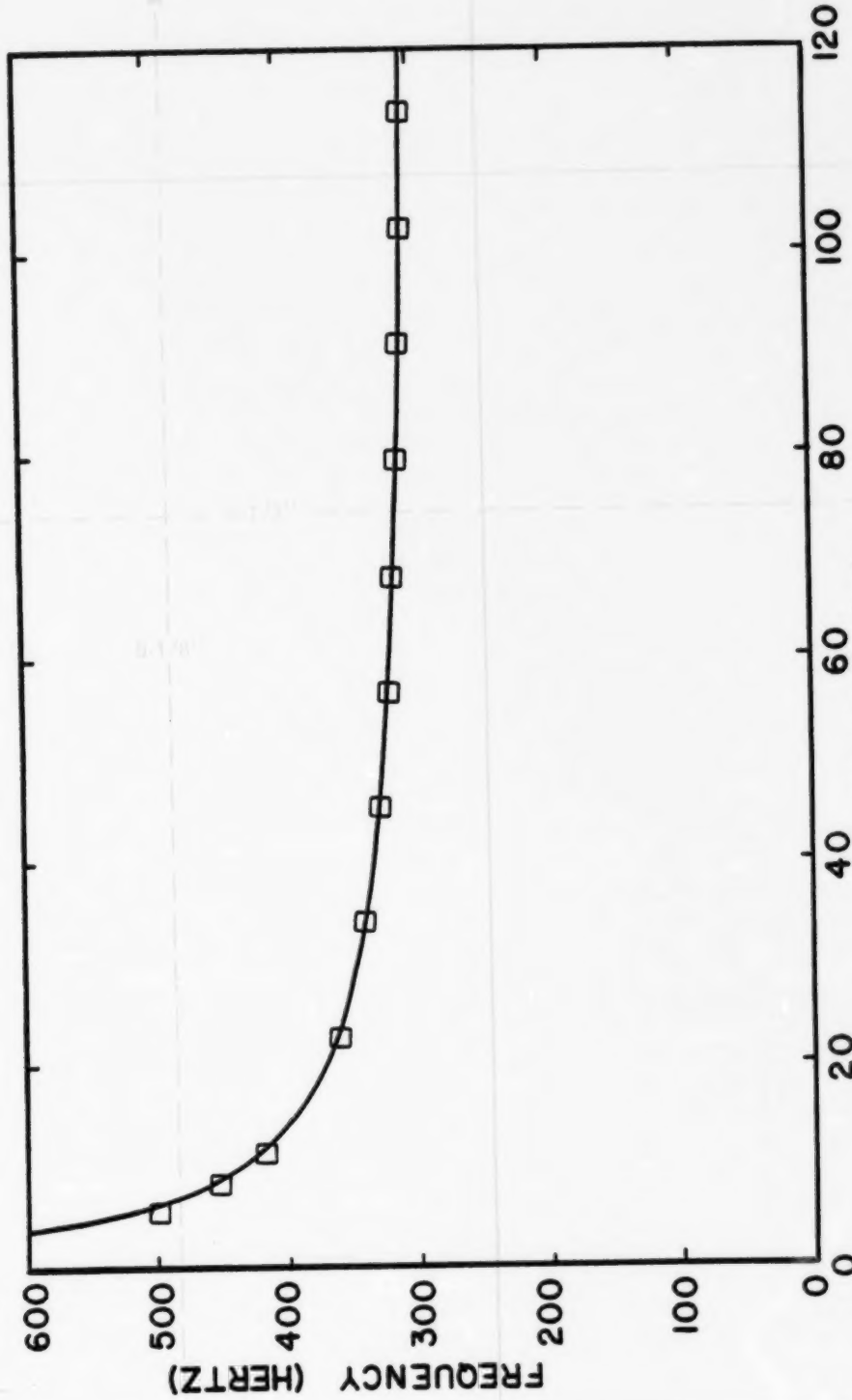

Figure 11. Plot of resonant frequency vs resonator volume for the Helmholtz cell.

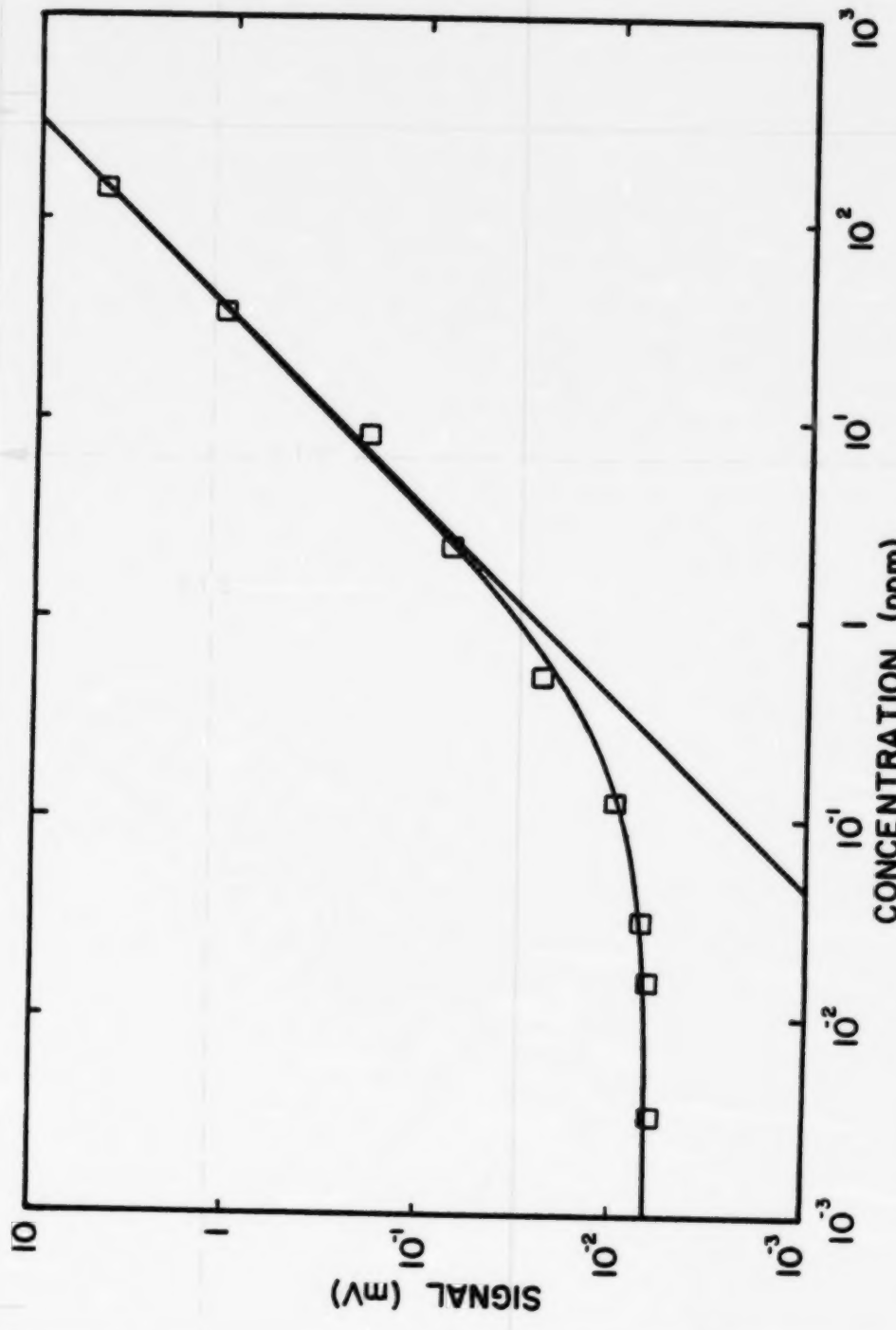

Figure 12. Plot of signal vs concentration of C_2H_4 in N_2 using the Helmholtz cell.

REFERENCES

1. E. L. Kerr and J. G. Atwood, Appl. Optics, 7, 915 (1968).

2. C. F. Dewey, Jr., R. D. Kamm and C. E. Hackett, Appl. Physics Letters, 23, 633 (1973).

3. E. Nodov, Appl. Optics, 17, 1110 (1978).

4. E. Max and L. G. Rosengren, Optics Communications, 11, 422, (1974).

5. E. S. Kritchman, S. Shtrikman and M. Slatkine, J. Op. Soc. Am, 68, 1257 (1978).

6. L. G. Rosengren, Infrared Physics, 13, 109 (1973).

7. L. G. Rosengren, Infrared Physics, 13, 173 (1973).

8. L. G. Rosengren, M. Erland and S. T. Eng. Journal of Physics E: Scientific Instruments, 7, 125 (1974).

9. L. G. Rosengren, Appl. Optics, 14, 1960 (1975).

10. C. W. Bruce, B. Z. Sojka, B. G. Hurd, W. R. Watkins, K. O. White and Z. Derzko, Appl. Optics, 15, 2970 (1976).

11. P. D. Goldan and K. Goto, Jour. Appl. Physics, 45, 4350 (1974).

12. Lord Rayleigh, Theory of Sound (vol. 2), Macmillan and Co. Ltd., New York, 1896.

13. R. R. Patty, G. W. Russwurm, W. A. McClenny, and D. R. Morgan, Appl. Optics, 13, 2850 (1974).